nature neuroscience

Single-neuron dynamics in human focal epilepsy

Wilson Truccolo[1–4,16], Jacob A Donoghue[1,16], Leigh R Hochberg[1,3–5], Emad N Eskandar[6,7], Joseph R Madsen[8,9], William S Anderson[9], Emery N Brown[10–12], Eric Halgren[13–15] & Sydney S Cash[1]

Epileptic seizures are traditionally characterized as the ultimate expression of monolithic, hypersynchronous neuronal activity arising from unbalanced runaway excitation. Here we report the first examination of spike train patterns in large ensembles of single neurons during seizures in persons with epilepsy. Contrary to the traditional view, neuronal spiking activity during seizure initiation and spread was highly heterogeneous, not hypersynchronous, suggesting complex interactions among different neuronal groups even at the spatial scale of small cortical patches. In contrast to earlier stages, seizure termination is a nearly homogenous phenomenon followed by an almost complete cessation of spiking across recorded neuronal ensembles. Notably, even neurons outside the region of seizure onset showed significant changes in activity minutes before the seizure. These findings suggest a revision of current thinking about seizure mechanisms and point to the possibility of seizure prevention based on spiking activity in neocortical neurons.

Seizures and epilepsy have been recognized since antiquity, yet we continue to struggle to define and understand these paroxysms of neuronal activity. Epileptic seizures are commonly considered to be the result of monolithic, hypersynchronous activity arising from an imbalance between excitation and inhibition in large populations of cortical neurons[1–3]. This view of ictal activity is highly simplified, and the level at which it breaks down is unclear. It is largely based on electroencephalogram (EEG) recordings, which reflect the averaged activity of millions of neurons. Whereas some *in vitro* studies have shown that sparse and asynchronous neuronal activity evolves into a single hypersynchronous cluster with elevated spiking rates at seizure initiation[4,5], as the canonical view would suggest, other animal model studies have supported a much less homogeneous progression in neuronal activity during seizures[6–8]. How well these animal models capture mechanisms operating in human epilepsy remains an open question[9,10]. Very few human studies have gone beyond macroscopic scalp and intracranial EEG signals to examine neuronal spiking underlying seizures[11–14]. Hence the behavior of single neurons in human epilepsy remains largely unknown.

The reliance on the macroscopic information of the EEG has also dominated attempts at discovering physiological changes preceding the seizure. The obvious goal of this approach is in predicting and then preventing seizures[15,16]. While *in vitro* and *in vivo* animal models suggest that different neuronal populations might have distinct roles during a preictal period[4–8,17–21], reliable seizure prediction based on detection of preictal changes in human scalp and intracranial EEG has remained elusive[16]. In addition, most seizures end abruptly and spontaneously, followed by a post-seizure attenuation in EEG activity[22]. The underlying mechanisms governing this behavior are also not understood. Various potential mechanisms, including among others, glutamate depletion, profound inhibition, modulatory effects from subcortical structures and depolarization block, have been hypothesized to underlie seizure termination[22,23]. Although these mechanisms clearly operate at the level of individual cells, to our knowledge, single-unit activity during this period has not been examined in humans. Such information could be useful in developing better strategies for seizure control and preventing status epilepticus[24].

A deeper understanding of neuronal spiking during the different phases of seizure generation would have profound implications for seizure prediction and may provide the basis for new and more effective therapies for people with epilepsy[25]. Here we studied the spiking activity of hundreds of neurons in four persons with focal epilepsy. We found significant changes in preictal activity in subsets of neurons. During seizure initiation and spread, we observed a high degree of heterogeneity in spiking activity. This heterogeneity did not seem to result purely from differences between interneurons and pyramidal cells; heterogeneity was present even within a class. Spiking evolved into a more homogeneous activity across the recorded neuronal ensemble toward seizure termination, during which we observed an almost complete cessation of spiking across the recorded cortical patch. Further, in our data, depolarization block did not seem to have a primary local role during the end of the seizure.

[1]Department of Neurology, Massachusetts General Hospital and Harvard Medical School, Boston, Massachusetts, USA. [2]Department of Neuroscience, Brown University, Providence, Rhode Island, USA. [3]Institute for Brain Science, Brown University, Providence, Rhode Island, USA. [4]Rehabilitation Research and Development Service, Department of Veterans Affairs, Providence, Rhode Island, USA. [5]School of Engineering, Brown University, Providence, Rhode Island, USA. [6]Department of Neurosurgery, Massachusetts General Hospital and Harvard Medical School, Boston, Massachusetts, USA. [7]Nayef Al-Rodhan Laboratories for Cellular Neurosurgery and Neurosurgical Technology, Massachusetts General Hospital and Harvard Medical School, Boston, Massachusetts, USA. [8]Department of Neurosurgery, Children's Hospital and Harvard Medical School, Boston, Massachusetts, USA. [9]Department of Neurosurgery, Brigham and Women's Hospital and Harvard Medical School, Boston, Massachusetts, USA. [10]Department of Anesthesia, Critical Care and Pain Medicine, Massachusetts General Hospital and Harvard Medical School, Boston, Massachusetts, USA. [11]Department of Brain and Cognitive Sciences, Massachusetts Institute of Technology, Cambridge, Massachusetts, USA. [12]Harvard-Massachusetts Institute of Technology, Division of Health Sciences and Technology, Massachusetts Institute of Technology, Cambridge, Massachusetts, USA. [13]Department of Radiology, University of California, San Diego, San Diego, California, USA. [14]Department of Neurosciences, University of California, San Diego, San Diego, California, USA. [15]Department of Psychiatry, University of California, San Diego, San Diego, California, USA. [16]These authors contributed equally to this work. Correspondence should be addressed to W.T. (wilson_truccolo@brown.edu).

Received 23 December 2010; accepted 15 February 2011; published online 27 March 2011; doi:10.1038/nn.2782

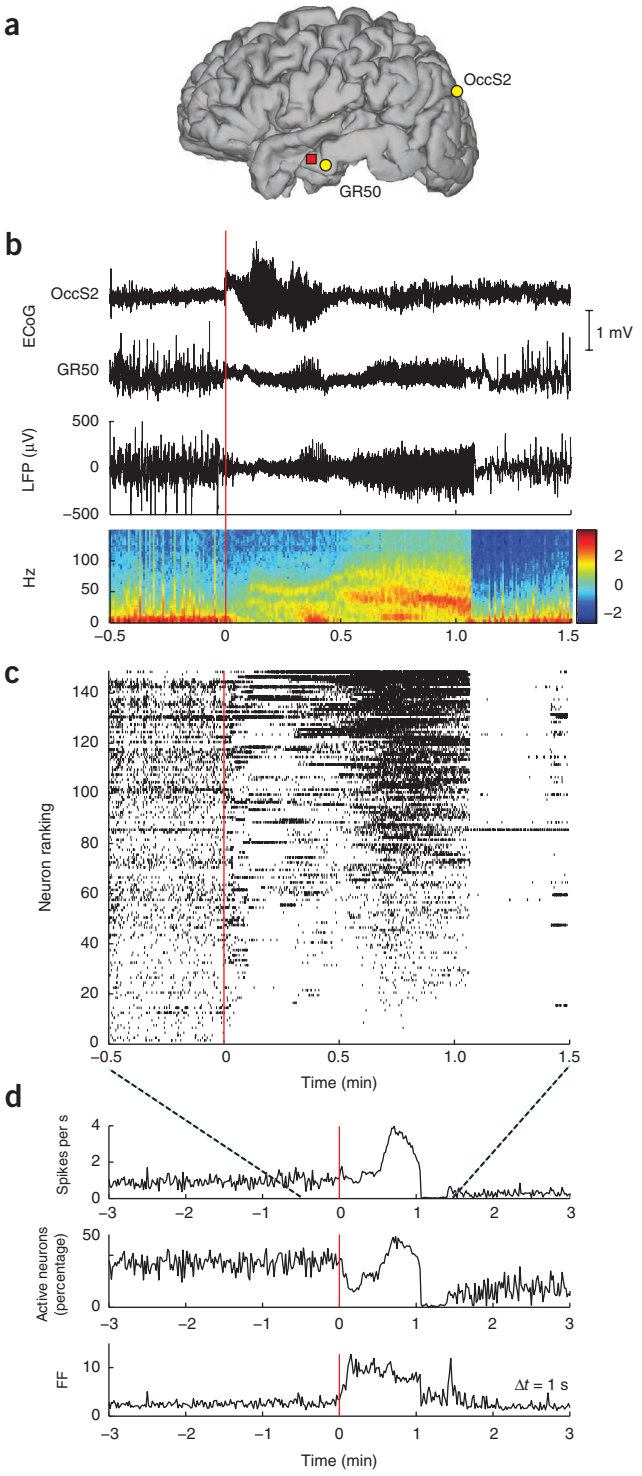

Figure 1 Heterogeneous neuronal spiking patterns during seizure. (**a**) Locations of the microelectrode array in participant A (red square), and subdural ECoG electrodes OccS2 and GR50 in occipital and middle temporal cortices, respectively. (**b**) ECoG traces recorded at the locations shown in **a** during seizure 1. The ECoG-based onset area was identified to be under the occipital electrode OccS2. Seizure onset is at time 0. The local field potential (LFP) recorded from a single channel in the microelectrode array and the corresponding spectrogram (in dB) are shown below. (**c**) Neuronal spike raster plot including all recorded neurons (n = 149). Each hash mark represents the occurrence of an action potential. Neurons were ranked (vertical axis) in increasing order according of their mean spiking rate during the seizure. (This ranking number is unrelated to physical location.) Toward the end of the seizure, activity across the population became more homogeneous until spiking was abruptly interrupted at seizure termination. With the exception of a few neurons, spiking in the recorded population remained suppressed for about 20 s. (**d**) The mean population rate, the percentage of active neurons and the Fano factor (FF) of the spike counts across different neurons at a given time (determined in 1-s time bins). These were roughly stationary during the several minutes preceding the seizure onset. An increase in the Fano factor, reflecting the heterogeneity in neuronal spiking, is observed around seizure onset and precedes an increase in the mean population rate.

RESULTS

We used specialized 96-channel microelectrode arrays[26–31] to record single-unit spiking activity and local field potentials from a 4 mm × 4 mm region of neocortex in four patients with epilepsy refractory to medical treatments. These patients were implanted with subdural grid electrodes to evaluate their cortical EEG activity (electrocorticogram; ECoG) and help localize the onset zone of their seizures for subsequent surgical resection. For research purposes, the microelectrode arrays were placed in addition to the grids (**Fig. 1**). We identified a total of 712 single-unit recordings in four participants (A, B, C and D). Single units were sorted using standard techniques (Online Methods). Although we recorded continuously over several days, the consistent sorting of single units over time periods longer than a few hours proved challenging. Over such long periods, waveforms of extracellularly recorded action potentials could change and units appear or disappear from recordings, owing perhaps to array micromotion, changes in brain states and other factors[32]. For this reason, for each analyzed session we identified for study those single units that were consistently recorded during a time period of ~2 h centered at the onset of each of eight seizures (see Online Methods). Microelectrode arrays in participants A (three seizures; n = 149, 131 and 131 single units recorded), B (two seizures; n = 57 in each) and D (n = 35 in one seizure) were placed in the middle temporal gyrus ~2 cm from the anterior tip. The microelectrode array in participant C (two seizures; n = 82 and 70) was placed in the middle frontal gyrus. Microelectrode arrays were positioned both within (participant C) and outside (~2–4 cm away; participants A, B and D) the seizure onset zone as subsequently defined by the ECoG-electrode locations at which the seizure first appeared (see Online Methods).

Heterogeneous neuronal spiking activity during seizures

Visual inspection of neuronal spike rasters revealed a variety of spiking patterns during seizure initiation, spread and maintenance (**Fig. 1c**; see also **Supplementary Fig. 1** and **Supplementary Movie 1** showing spiking rates on the microelectrode array). For example, whereas some neurons increased their spiking rates near the seizure onset, others decreased. These transient spiking rate modulations occurred at different times for different groups of neurons. The Fano factor (variance divided by the mean) of the single neuron spike counts across the population at a given time during the seizure (1-s time bins), which gives an index of spiking heterogeneity in the ensemble, increased substantially after the seizure onset—in some seizures by fivefold (**Fig. 1d**).

This diversity of neuronal modulation patterns was observed to a greater or lesser extent in all seizures and participants studied (**Supplementary Figs. 1–4**). Such heterogeneity in spiking rate modulation patterns directly challenges the canonical characterization of epileptic seizures as a simple, widespread and homogeneous runaway

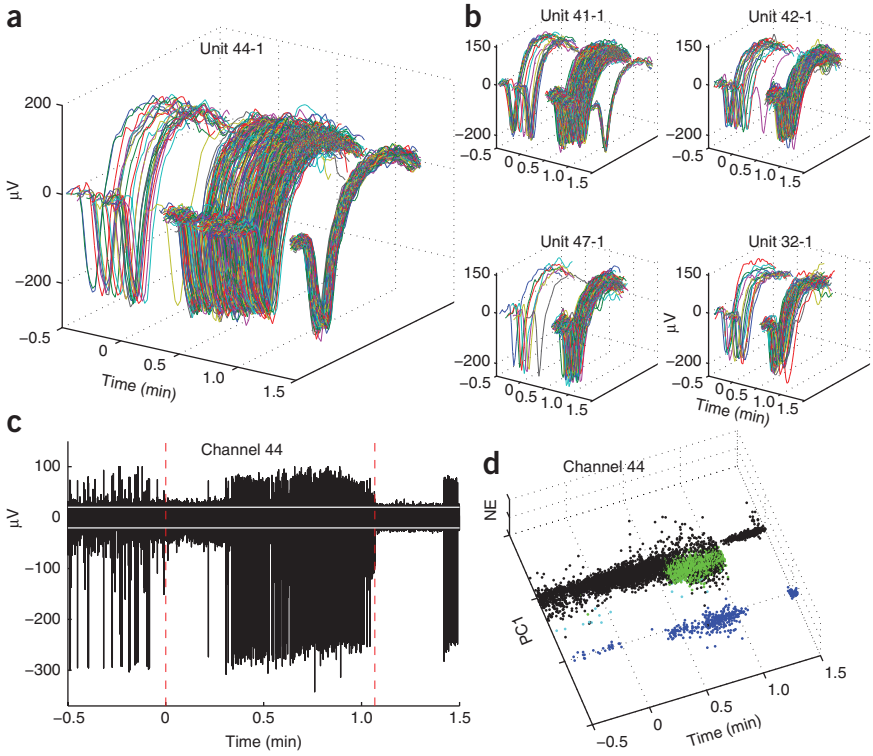

Figure 2 Transient suppression of neuronal spiking during the seizure and at seizure termination. (**a**) Spike waveforms from neuron 44-1 (participant A, seizure 1; neuron ranked no. 131 in **Fig. 1c**). Spiking stopped for ~ 20 s during the initial seizure phase. The lack of major changes in spike waveform and preceding low spiking rate suggest that suppression was not due to sorting artifacts or depolarization block. (**b**) Four examples of units with similar behavior, recorded from different sites. All five units were classified as putative principal cells. (**c**) The high-pass filtered potentials recorded at electrode 44. Larger spikes correspond to unit 44-1, shown in **a**. Dashed vertical lines show seizure onset and termination, respectively. White lines mark ±3 s.d. of the background noise, estimated from the 'silent' period after seizure termination. Another unit with smaller extracellularly recorded action potentials intensifies spiking during the 0.5–1.1 min interval. After seizure termination, both single-unit and multiunit activity were suppressed and the recorded potentials correspond primarily to background noise. Although there is some gradual decrease in spike amplitudes, this decrease is much smaller than what would be expected from depolarization block. See **Supplementary Figure 2** for channels 32, 41, 42 and 47. (**d**) Projection of thresholded waveforms onto a feature space shows clearly separable units. Blue dots represent thresholded spikes from unit 44-1; PC1 and NE denote the first principal component and a nonlinear energy feature, respectively. Green dots correspond to a smaller unit. Black dots correspond to thresholded noise and unsorted multiunit spikes.

excitation leading to a hypersynchronized state. Heterogeneity was present regardless of whether the seizure initiated near (participant C) or far from (the other three participants) the location of the microelectrode array. The admixture of different spiking patterns suggests that heterogeneity is not purely propagation driven but must also reflect local network properties. As based on the Fano factor, this heterogeneity was higher during seizure initiation and decreased toward seizure termination (**Fig. 1d** and **Supplementary Fig. 1**).

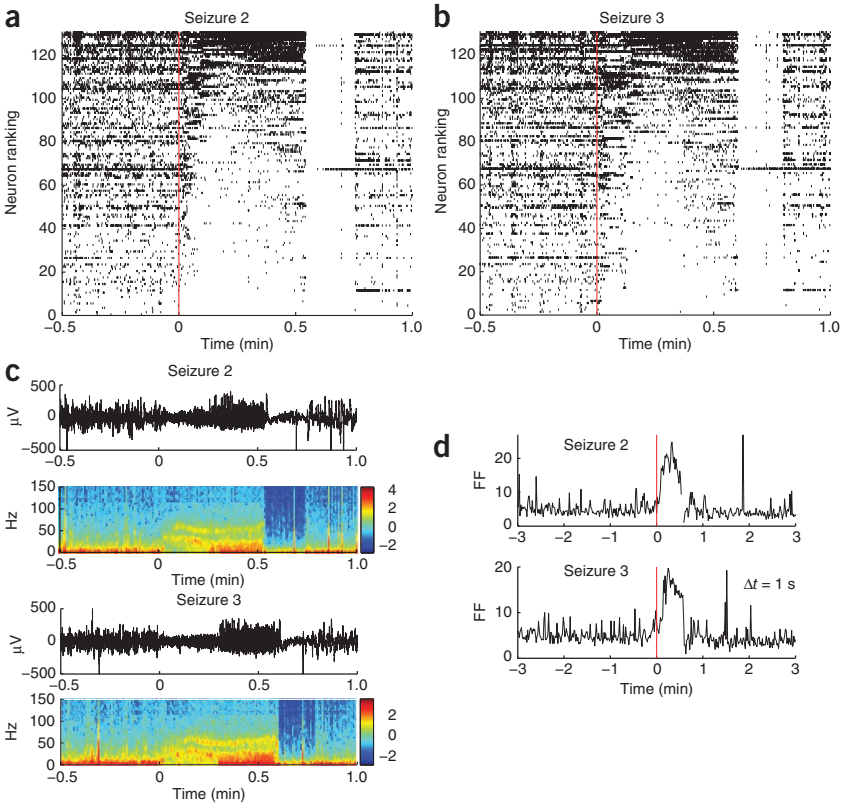

Figure 3 Reproducibility of neuronal spiking modulation patterns across consecutive seizures. (**a**,**b**) An example from participant A with 131 neurons. Following conventions used in **Figure 1c**, neurons are ranked according to their mean rates measured during the seizure. Seizure 3 (**b**) follows the same ranking as seizure 2 (**a**); that is, the single units in any given row of seizures 2 and 3 are the same. Most neurons coarsely preserved the types of spiking rate modulation across the two seizures. For example, the lowest-ranked neurons decreased or stopped spiking; and many of the top-ranked neurons presented similar transient increases in spiking rate modulation. As in seizure 1 (**Fig. 1**), an almost complete suppression of spiking in the neuronal population occurred abruptly at seizure termination. (**c**) The corresponding low-pass filtered local field potentials (LFPs) and spectrograms (from the same microelectrode array channel shown in **Fig. 1**; power in dB). (**d**) The Fano factor for the spike counts (1-s time bins) in the population of recorded neurons showed similar increase during both seizures, reflecting the increased heterogeneity in neuronal spiking across the population.

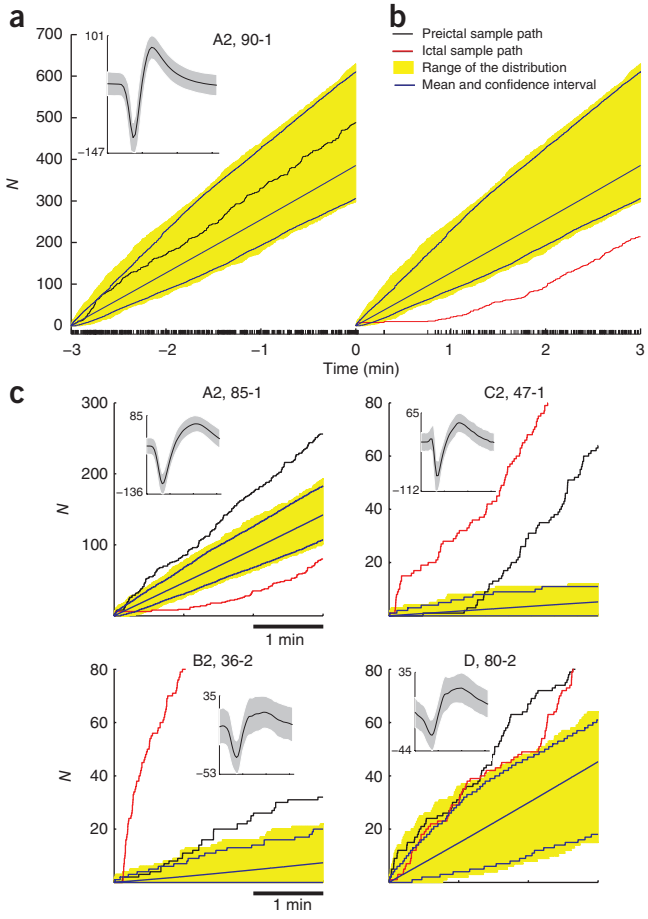

Figure 4 Preictal and ictal modulations in spiking rates. (**a**) The neuronal spiking sample path *N* (neuron 90-1; A2: participant A, seizure 2). The corresponding spike train is shown at the bottom and the inset shows the mean ± 2 s.d. of all recorded spike waveforms. Seizure onset corresponds to time 0. For comparison purposes, the initial value of the sample path is set to 0. The yellow band corresponds to the range of the 3-min-long sample paths observed during a 30-min interictal period preceding the preictal period. Interictal sample paths in this distribution were obtained from an overlapping 3-min-long moving time window, stepped 1 s at a time. Blue curves and surrounding yellow band correspond to the average interictal sample path and the 95% confidence interval, respectively. A sample path was judged to have deviated from the interictal sample paths when it fell outside the range of the collection of interictal sample paths at any given time. (**b**) Neuron 90-1 transiently stopped spiking for tens of seconds just after the seizure onset. As expected, the sample path during the seizure did deviate from the observed interictal paths. The neuron's spiking rate gradually recovered and eventually settled at the typical mean rate. (**c**) Four examples of preictal and ictal sample path deviations, one for each participant. Note that although the preictal and ictal sample paths are plotted along the same axis, they refer to a 3-min period before and after, respectively, the seizure onset.

Seizure termination and suppression of neuronal spiking

In contrast to the beginning of the seizure, seizure termination in participants A, B and C involved widespread, complete cessation of activity for most recorded neurons (**Fig. 1c** and **Supplementary Figs. 1**,**3**). Spiking activity remained suppressed for several seconds (ranging from 5 to 30 s) after seizure termination, until more normal spiking rates gradually returned. Decreases in spiking activity (particularly during either initial or final stages of the seizure) were not due to sorting artifacts such as spike dropout because of obvious alterations in spike waveform. Changes in spike waveforms can be induced by, for example, intense bursting activity. In contrast, **Figure 2a**,**b** shows several examples of units that almost completely ceased spiking for 20–30 s after seizure onset, yet did not present any obvious changes in waveform shape and amplitude that would result in spike dropout. Furthermore, toward the end of the seizure, the same units increased substantially their spiking rates, showing that we were still able to detect their spiking even at much higher spiking rates.

Notably, it also seems that the suppression of these units' spiking either during seizure maintenance or at the end of the seizure was not due to a typical depolarization block scenario[18,19,23] where neuronal spike amplitudes decrease gradually until they cannot be detected or spiking is blocked. For example, the examination of the high-pass-filtered potentials (**Fig. 2c**,**d**) shows that unit 44-1 stopped spiking at a point where peak-to-peak waveform amplitudes were about 300 μV, whereas the threshold for spike detection was set at around −30 μV. (Examples for other neurons are shown in **Supplementary Fig. 2**).

Reproducibility of spike patterns in consecutive seizures

In participants A and B, two consecutive seizures occurred within a period of about an hour. In these cases, we were able to ensure that the same units were recorded and consistently identified during both seizures (see Online Methods). This permitted us to examine the reproducibility of neuronal spiking patterns across seizures. For instance, even though the third seizure in participant A lasted slightly longer than the second, the same motifs in the neuronal spiking patterns recurred (**Fig. 3**). The Pearson correlation coefficient (a measure of similarity) between two spike trains during the initial 30 s of each seizure, for each neuron and averaged across the population, was 0.82. Similar observation was also made for the two consecutive seizures in participant B, with an average correlation coefficient of 0.72 (**Supplementary Fig. 3**), suggesting a high degree of similarity in both seizures. The probability that these correlation coefficients were statistically zero was extremely small ($P < 10^{-6}$; see Online Methods).

We also examined how the similarity between the two ictal events compared to the similarity of random interictal segments preceding the two corresponding consecutive seizures. A random resampling approach using interictal spike rasters each lasting 30 s resulted in significantly smaller correlation coefficients; that is, coefficients whose 95% confidence intervals (mean ± 2 s.d.) corresponded to 0.45 ± 0.14 and 0.16 ± 0.25 for participants A and B, respectively. Despite general similarities across seizures, there were also notable differences in the fraction of active neurons in the population. For example, whereas these fraction increased after a transient decrease at seizure onset in seizure 1 (participant A; **Fig. 1d**), throughout seizures 2 and 3 it remained lower than during the preictal period (**Supplementary Fig. 4**).

Preictal and ictal changes in neuronal spiking activity

To characterize preictal and ictal changes in spiking rates, we represented a single neuron's spike train as a sample path[33]. A sample path consists of the cumulative number of neuronal spikes as a function of time (**Fig. 4a**). The sample path representation allows us to preserve information about transient changes in instantaneous spiking rates. We asked whether an observed sample path for a given neuron during the preictal or ictal periods deviated from the collection of sample paths of same time length observed during a preceding interictal period. In this way, we were able to detect

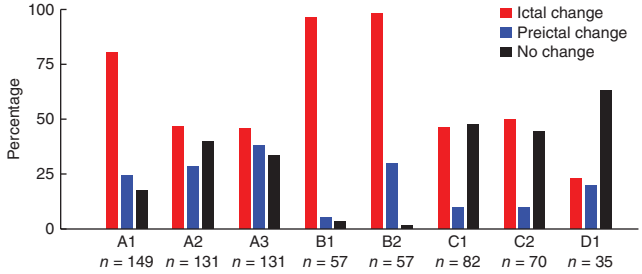

Figure 5 Preictal and ictal sample path deviations with respect to an interictal period. Each bar indicates the percentage of preictal and ictal sample path deviations in the recorded neuronal population, for each participant and seizure. Sample paths and sample path deviations were defined as in **Figure 4**.

transient increases or decreases in spiking rate that were atypical with respect to the preceding interictal activity (**Fig. 4b**,**c**).

We found that substantial numbers of neurons significantly changed their activities as the seizure approached. The percentage of neuronal recordings that showed a preictal deviation varied from 20% (7/35, participant D) to 29.9% (123/411, participant A). The percentages of neurons that showed preictal and/or ictal changes are specified separately for each participant and seizure in **Figure 5**. Observed deviations consisted either of increases or decreases in spiking rate. Across all participants and seizures (712 recordings), 11.8% of recorded neurons increased their spiking rate during the preictal period, and 7.5% decreased. In many cases the onset time for the deviation was earlier than 1 min before the seizure onset time (**Fig. 4c**). This finding suggests that changes in neuronal spiking activity, even for single neurons recorded well outside the identified epileptic focus, may be detected minutes before the seizure onset defined by ECoG inspection. Several neurons in participants A showed consistent sample path deviations across seizures 2 and 3, the two consecutive seizures where the same single units were recorded (**Supplementary Fig. 5**).

The percentage of neuronal recordings that showed a sample path deviation during the ictal period varied from 22.8% (8/35, participant D) to 97.4% (111/114, participant B). In line with the heterogeneity observed in raster plots, several types of deviations were observed during the seizure—all from single units recorded simultaneously from a small cortical patch (encompassing different cortical columns). Across all participants and seizures, 45.4% and 9.9% of the neuronal recordings increased and decreased, respectively, their spiking rates during the seizure. Furthermore, a few neurons showed a transient increase (0.1%) followed by a transient decrease in spiking rates, or vice-versa (1.3%). Overall, we found fifteen different patterns of neuronal modulation when taking into consideration both preictal and ictal patterns. (See **Supplementary Table 1** for detailed percentages for each participant and seizure.) In addition to these types of sample path deviations, a few neurons in participant A also showed much slower and larger modulations in spiking rates that preceded the seizure onset by tens of minutes (**Supplementary Fig. 6**) and were not correlated with obvious behavioral or state changes.

Neurons that showed preictal and ictal modulation in spiking rates tended to have statistically higher bursting rates during interictal periods (Kruskal-Wallis test, $P < 0.01$, Tucker-Kramer correction for multiple comparisons; see Online Methods and **Supplementary Figs. 7** and **8**). Furthermore, in participant A, the single units recorded could be classified into putative interneurons and principal neurons according to spike half-width and peak-to-valley time width features (see Online Methods and **Supplementary Fig. 9**; waveforms from the other three participants formed a homogeneous cluster in each case). On the basis of this classification, 79% (45/57) and 68% (240/354) of interneurons and principal cells recordings, respectively, showed some type of preictal or ictal modulation. In addition, the fraction of recorded interneurons that showed a preictal increase was 60% larger than the corresponding fraction of principal neurons (χ^2 test, $P < 10^{-6}$, with Bonferroni correction for multiple comparisons; see **Supplementary Fig. 10**).

Specificity of preictal changes in neuronal activity

The observed sample path deviations during the preictal period could simply reflect spontaneous or evoked modulations of spiking activity unrelated to the upcoming seizure. Therefore, we also examined how often such sample path deviations could occur during interictal periods. This analysis also provides a preliminary assessment of the specificity of a very simple seizure prediction algorithm that, for example, predicted a seizure every time an observed number of deviations across the recorded neuronal population exceeded a specified threshold. Specifically, we estimated the probability of observing a given number (percentage) of such sample path deviations across the neuronal population during interictal periods. Three different interictal periods were used for participant A, two for participants B and C, and one for participant D. A 3-min-long segment was then randomly selected from a given interictal period and a corresponding (target) sample path was computed for each neuron. Next, we checked whether each sample path deviated from its corresponding distribution derived from paths of same length sampled from a 30-min interictal segment, as done before in **Figure 4**. This 30-min segment was adjacent to but nonoverlapping with the randomly selected target sample path. The entire procedure was repeated hundreds of times to obtain a distribution of the percentage of deviations across the recorded neuronal population during a given interictal period. Finally, a threshold was defined based on the average number of preictal deviations across the examined seizures for a given participant. (For example, the threshold for participant A was derived from the mean of the percentage of neurons that showed a preictal deviation across the three seizures; **Fig. 5**.) Given this threshold and a distribution of percentage of deviations, we could then compute the probability that a given percentage of observed deviations across the population during an interictal period was smaller than the specified threshold. As mentioned above, this probability provides an estimate of the specificity of a seizure prediction algorithm based on the defined sample path deviations.

With the exception of participant C, for whom interictal activity showed a very high rate of epileptiform events consisting of slow neuronal bursting and ECoG spike and wave discharges, promising specificity results (0.78–0.94) were obtained for participants A, B and D (**Supplementary Fig. 11**). Despite these positive preliminary results, we emphasize that a more conclusive assessment will require much larger data sets, to probe a larger range of physiological and behavioral states, as well as corresponding sensitivity analyses.

DISCUSSION

Our findings, based on the most extensive description of single-unit activity in human neocortical seizures yet reported, reveal several important and heterodox points about the nature of epileptic activity. First, the observed heterogeneity in neuronal behavior argues against homogeneous runaway excitation or widespread paroxysmal depolarization as the primary mechanism underlying seizure initiation. Rather, our data indicate that seizures result from a complex interplay among groups of neurons that present different types of spiking

behaviors evolving at multiple temporal and spatial scales. We have also observed similar heterogeneity in interictal discharges[31]. Given the 1-mm microelectrode length, it is likely we recorded from cells in layers 3 and 4. Several studies[5,34,35] suggest that epileptiform activity involves and is perhaps initiated by cells in layer 5. Although the potential role of these cells needs to be further explored, they do not seem to be driving homogenous activity. Furthermore, because of the nature of these recordings, we might not have recorded from the initiation site in any of the participants (including participant C). As a result, it is possible that a different form of neuronal dynamics would be observed at the 'focus'. This is especially likely to be the case in a region of dysplasia in which the neurons and their layering are severely abnormal.

Heterogeneity in neuronal spiking activity during seizures has been previously observed in animal model studies[6–8]. In particular, it has been hypothesized[7] that such heterogeneity could reflect three main sequential stages or states during seizure spreading: 'depressed', 'projected' and 'propagated' states. The fact that the heterogeneity reported here in human epilepsy appears simultaneously in small patches of neocortex would speak against this hypothesis; or, alternatively, it would require that different groups of neurons entered and dwelled in different states with different time constants, perhaps owing to differences in initial conditions or in intrinsic and local network dynamical properties. In addition, our finding based on the classification of units into putative principal cells and interneurons, namely that some putative pyramidal cells increased while other decreased their spiking rates, suggests that such heterogeneity does not simply reflect interleaved spiking of pyramidal cells and interneurons[18,19]. We also speculate that the observed heterogeneity in the neuronal collective dynamics[30] could result from fragmentation into multicluster synchronization, which has been studied in various dynamical systems[36]. The fact that such diverse spiking activity underlies seemingly 'monomorphic' EEG waveforms raises the possibility that even normal cortical rhythms might also reflect very heterogeneous underlying neuronal ensemble spiking.

Second, one of the noteworthy features of these data was the abrupt and widespread suppression of neuronal action potentials at seizure end. In participant A, for example, spiking of both putative interneurons and principal neurons became suppressed. Previous work has suggested that seizures might self-terminate because of depolarization block resulting from changes in ionic concentrations in the extracellular space. A depolarization block of neuronal spikes due to a chain of events that ends with astrocytic release of large amounts of potassium has been hypothesized[23]. However, several units became suppressed at seizure termination without showing typical signatures of depolarization block (**Fig. 2**)—an indication that depolarization block was not the primary local factor responsible for the observed marked suppression in spiking activity. Furthermore, our results also argue against massive inhibition from a local source because the suppression of neuronal spiking affected both putative interneurons and other principal cells. Alternatively, distant modulatory inputs involving subcortical structures—for example, thalamic nuclei or substantia nigra pars reticulata[22]—could lead to seizure termination. There is also the possibility that this critical transition could arise from an emergent property of the large-scale network itself leading to spatially synchronous extinction[37].

From a therapeutic perspective, our analysis demonstrates, for the first time in humans, that preictal neuronal spiking reflects a distinct and widely occurring physiological state in focal epilepsies. This is true even outside the region of seizure initiation, suggesting that it may be possible to obtain predictive information from individual neuronal activity without necessarily localizing what has been traditionally considered the seizure focus. Substantiation of this possibility will require large data sets, perhaps only available through multisite collaborative efforts, containing sufficient interictal data for proper specificity and sensitivity analyses[16]. Promisingly, our data suggests that the clinical care of patients with epilepsy could be revolutionized by using dynamics of ensembles of single neurons to predict seizures.

METHODS

Methods and any associated references are available in the online version of the paper at http://www.nature.com/natureneuroscience/.

Note: Supplementary information is available on the Nature Neuroscience website.

ACKNOWLEDGMENTS

The authors thank the patients who participated in this study, as well as the nursing and physician staff at each facility. We also thank A.M. Chan, C.J. Keller, A. Dykstra and J.E. Cormier for technical assistance, and J.P. Donoghue and K.J. Staley for critical reading of the manuscript. This research is funded by a CIMIT grant and US National Institutes of Health (NIH) National Institute of Neurological Disorders and Stroke (NINDS) NS062092 to S.S.C.; an NIH–NINDS Career Award (5K01NS057389) to W.T.; NIH NS018741 to E.H.; NINDS K08NS066099-01A1 to W.S.A.; US National Eye Institute EY017658, US National Institute on Drug Abuse NS063249, US National Science Foundation IOB 0645886, Howard Hughes Medical Institute and the Klingenstein Foundation to E.N.E.; NIH Director's Pioneer Award DP1OD003646 to E.N.B.; US Department of Veterans Affairs Career Development Transition Award, Doris Duke Charitable Foundation–Clinical Scientist Development Award, Massachusetts General Hospital–Deane Institute for Integrated Research on Atrial Fibrillation and Stroke, and NIH-NIDCD R01DC009899 to L.R.H. The contents do not represent the views of the Department of Veterans Affairs or the United States government.

AUTHOR CONTRIBUTIONS

W.T., S.S.C. and J.A.D. wrote the paper. W.T. and J.A.D. conducted the data analysis. Data collection and preprocessing were done by J.A.D., W.T. and S.S.C. S.S.C., L.R.H., W.T. and E.H. conceived and planned the research. E.N.B. provided guidance on methods of data analysis and interpretation. E.N.E., W.S.A. and J.R.M. performed the surgeries and microelectrode array implantations. All authors participated in editing the manuscript.

COMPETING FINANCIAL INTERESTS

The authors declare competing financial interests: details accompany the full-text HTML version of the paper at http://www.nature.com/natureneuroscience/.

Published online at http://www.nature.com/natureneuroscience/.
Reprints and permissions information is available online at http://npg.nature.com/reprintsandpermissions/.

1. Penfield, W.G. & Jasper, H.H. *Epilepsy and the Functional Anatomy of the Human Brain* (Little, Brown, Boston, 1954).
2. Schwartzkroin, P.A. Basic mechanisms of epileptogenesis. in *The Treatment of Epilepsy* (ed. Wyllie, E.) 83–98 (Lea and Febiger, Philadelphia, 1993).
3. Fisher, R.S. *et al.* Epileptic seizures and epilepsy: definitions proposed by the International League Against Epilepsy (ILAE) and the International Bureau for Epilepsy (IBE). *Epilepsia* **46**, 470–472 (2005).
4. Jiruska, P. *et al.* High-frequency network activity, global increase in neuronal activity, and synchrony expansion precede epileptic seizures *in vitro*. *J. Neurosci.* **30**, 5690–5701 (2010).
5. Pinto, D.J., Patrick, S.L., Huang, W.C. & Connors, B.W. Initiation, propagation, and termination of epileptiform activity in rodent neocortex *in vitro* involve distinct mechanisms. *J. Neurosci.* **25**, 8131–8140 (2005).
6. Matsumoto, H. & Ajmone Marsan, C. Cortical cellular phenomena in experimental epilepsy: ictal manifestations. *Exp. Neurol.* **9**, 305–326 (1964).
7. Sawa, M., Nakamura, K. & Naito, H. Intracellular phenomena and spread of epileptic seizure discharges. *Electroencephalogr. Clin. Neurophysiol.* **24**, 146–154 (1968).
8. Bower, M. & Buckmaster, P.S. Changes in granule cell firing rates precede locally recorded spontaneous seizures by minutes in an animal model of temporal lobe epilepsy. *J. Neurophysiol.* **99**, 2431–2442 (2008).
9. Jefferys, J.G.R. Models and mechanisms of experimental epilepsies. *Epilepsia* **44** (suppl. 12): 44–50 (2003).
10. Buckmaster, P.S. Laboratory animal models of temporal lobe epilepsy. *Comp. Med.* **54**, 473–485 (2004).

11. Halgren, E., Babb, T.L. & Crandall, P.H. Post-EEG seizure depression of human limbic neurons is not determined by their response to probable hypoxia. *Epilepsia* **18**, 89–93 (1977).
12. Wyler, A.R., Ojemann, G.A. & Ward, A.A. Jr. Neurons in human epileptic cortex: correlation between unit and EEG activity. *Ann. Neurol.* **11**, 301–308 (1982).
13. Babb, T.L., Wilson, C.L. & Isokawa-Akesson, M. Firing patterns of human limbic neurons during stereoencephalography (SEEG) and clinical temporal lobe seizures. *Electroencephalogr. Clin. Neurophysiol.* **66**, 467–482 (1987).
14. Engel, A.K., Moll, C.K.E., Fried, I. & Ojeman, G.A. Invasive recordings from the human brain: clinical insights and beyond. *Nat. Rev. Neurosci.* **6**, 35–47 (2005).
15. Lopes da Silva, F.H. *et al.* Dynamical diseases of brain systems: different routes to epilepsy. *IEEE Trans. Biomed. Eng.* **50**, 540–548 (2003).
16. Mormann, F., Andrzejak, R.G., Elger, C.E. & Lehnertz, K. Seizure prediction: the long and winding road. *Brain* **130**, 314–333 (2007).
17. Bragin, A., Engel, J. Jr., Wilson, C.L., Fried, I. & Mathern, G.W. Hippocampal and entorhinal cortex high-frequency oscillations (100–500 Hz) in human epileptic brain and in kainic acid-treated rats with chronic seizures. *Epilepsia* **40**, 127–137 (1999).
18. Bikson, M., Hahn, P.J., Fox, J.E. & Jefferys, J.G.R. Depolarization block of neurons during maintenance of electrographic seizures. *J. Neurophysiol.* **90**, 2402–2408 (2003).
19. Ziburkus, J., Cressman, J.R., Barreto, E. & Schiff, S.J. Interneuron and pyramidal cell interplay during in vitro seizure-like events. *J. Neurophysiol.* **95**, 3948–3954 (2006).
20. Cymerblit-Sabba, A. & Schiller, Y. Network dynamics during development of pharmacologically induced epileptic seizures in rats in vivo. *J. Neurosci.* **30**, 1619–1630 (2010).
21. Yaari, Y. & Beck, H. "Epileptic neurons" in temporal lobe epilepsy. *Brain Pathol.* **12**, 234–239 (2002).
22. Lado, F.A. & Moshe, S.L. How do seizures stop? *Epilepsia* **49**, 1651–1664 (2008).
23. Bragin, A., Penttonen, M. & Buzsaki, G. Termination of epileptic afterdischarge in the hippocampus. *J. Neurosci.* **17**, 2567–2579 (1997).
24. Treiman, D.M. Status epilepticus. in *The Treatment of Epilepsy: Principles and Practice.* (ed. Wyllie, E.) 681–697 (Lippincott Williams & Wilkins, Philadelphia, 2001).
25. Jacobs, M.P. *et al.* Curing epilepsy: progress and future directions. *Epilepsy Behav.* **14**, 438–445 (2009).
26. Hochberg, L.R. *et al.* Neuronal ensemble control of prosthetic devices by a human with tetraplegia. *Nature* **442**, 164–171 (2006).
27. Truccolo, W., Friehs, G.M., Donoghue, J.P. & Hochberg, L.R. Primary motor cortex tuning to intended movement kinematics in humans with tetraplegia. *J. Neurosci.* **28**, 1163–1178 (2008).
28. Schevon, C.A. *et al.* Microphysiology of epileptiform activity in human neocortex. *J. Clin. Neurophysiol.* **25**, 321–330 (2008).
29. Kim, S.-P., Simeral, J.D., Hochberg, L.R., Donoghue, J.P. & Black, M.J. Neural control of computer cursor velocity by decoding motor cortical spiking activity in humans with tetraplegia. *J. Neural Eng.* **5**, 455–476 (2008).
30. Truccolo, W., Hochberg, L.R. & Donoghue, J.P. Collective dynamics in human and monkey sensorimotor cortex: predicting single neuron spikes. *Nat. Neurosci.* **13**, 105–111 (2010).
31. Keller, C.J. *et al.* Heterogeneous neuronal firing patterns during interictal epileptiform discharges in the human cortex. *Brain* **133**, 1668–1681 (2010).
32. Santhanam, G. *et al.* Hermes B: a continuous neural recording system for freely behaving primates. *IEEE Trans. Biomed. Eng.* **54**, 2037–2050 (2007).
33. Truccolo, W., Eden, U.T., Fellows, M.R., Donoghue, J.P. & Brown, E.N. A point process framework for relating neural spiking activity to spiking history, neural ensemble and extrinsic covariate effects. *J. Neurophysiol.* **93**, 1074–1089 (2005).
34. Connors, B.W. Initiation of synchronized neuronal bursting in neocortex. *Nature* **310**, 685–687 (1984).
35. Ulbert, I., Heit, G., Madsen, J., Karmos, G. & Halgren, E. Laminar analysis of human neocortical interictal spike generation and propagation: current source density and multiunit analysis in vivo. *Epilepsia* **45** (suppl. 4): 48–56 (2004).
36. Amritkar, R.E. & Rangarajan, G. Stability of multicluster synchronization. *Int. J. Bifurc. Chaos* **19**, 4263–4271 (2009).
37. Amritkar, R.E. & Rangarajan, G. Spatially synchronous extinction of species under external forcing. *Phys. Rev. Lett.* **96**, 258102 (2006).

ONLINE METHODS

Participants, clinical electrodes and recordings. Four patients (A, B, C and D, ages 21–52 years (mean 29.7), three women) with medically intractable focal epilepsy underwent clinically indicated intracranial cortical recordings using grid electrodes for epilepsy monitoring[38,39]. Clinical electrode implantation, positioning, duration of recordings and medication schedules were based purely on clinical need as judged by an independent team of clinicians. Patients were implanted with intracranial subdural grids, strips and/or depth electrodes (Adtech Medical Instrument Corporation) for 5–10 d in a specialized hospital setting until data sufficiently identified the seizure focus for appropriate resection. Continuous intracranial EEG was recorded with standard recording systems (XLTEK) and captured many seizures. Seizure onset times were determined by an experienced encephalographer (S.S.C.) through inspection of ECoG recordings, referral to the clinical report of the ECoG and clinical manifestations recorded on video. The number of seizures varied across the participants. Owing to operational issues, not all of these seizures were recorded or provided data with a high signal-to-noise ratio. Among data sets with clearly separable single units, we selected eight different seizures among the four participants. All steps of the analysis of intracranial EEG data were performed using Neuroscan Edit software (Compumedics) and custom designed Matlab (MathWorks) software.

Participant A. Participant A was a right-handed woman 52 years old at the time of the continuous 8-d video and invasive EEG monitoring study. She had a history of complex partial seizures with occasional secondary generalization beginning at the age of 4 and typically suffered from 10–15 events per day. Her seizures usually presented with sudden speech arrest associated with confusion and repetition of the activity she was doing just before the onset of the seizure. Magnetic resonance imaging (MRI) showed a large lesion in the left hemisphere extending from the occipital region to the temporal region, which was consistent with encephalomalacia. Moreover, a positron-emission tomography (PET) scan showed hypometabolism in the left occipital, temporal and parietal regions. On the basis of these findings, the patient was implanted with a combination of a subdural grid and strip electrodes and depth electrodes over the left hemisphere. The NeuroPort microelectrode array was placed in the middle temporal gyrus in a region of cortex nearly certain to be resected. The distance to the nearest ECoG electrode where seizure onsets were detected was ~2 cm.

There were several seizures throughout the recordings; all lasted about 1 min or less and had a similar electrographic pattern. They typically began with low-amplitude, fast activity—up to 300 μV, ~30 Hz—in an anterior temporal strip, sometimes with an associated burst of polyspike activity in an occipital strip, or began at an occipital site (**Fig. 1**). Simultaneously, there was a generalized suppression of the grid activity beginning in the posterior inferior quadrant and then spreading to encompass the entire grid. After the onset, there was a buildup of high frequencies and higher amplitudes (up to 500 μV) in the posterior inferior quadrant and occipital region. Sometimes, rhythmic ECoG spikes occurred in the anterior temporal strip and posterior temporal depths.

At the conclusion of the study the patient underwent resection of the left anterior temporal lobe. Pathology showed hippocampal sclerosis with secondary cortical gliosis. The patient remained seizure free for 1 year after the resection, but seizures returned after this period.

Participant B. Participant B was a right-handed man 21 years old at the time of the continuous 8-d video and invasive EEG monitoring study. He had suffered from seizures since at least age 15. Most of his events were characterized by a blank stare and oral automatisms accompanied by stiffening and posturing of the right hand. He was implanted with a series of strip electrodes covering the left frontal and temporal regions. The NeuroPort array was placed in the middle temporal gyrus about 1–2 cm posterior to the temporal tip. The distance to the nearest ECoG electrode where seizure onsets were detected was ~2 cm. Sharp waves were observed interictally in the posterior temporal regions. Four seizures, all with similar clinical and electrographic features, were recorded. Seizures were characterized by a left gaze preference and tonic and then clonic movements of the right arm. Electrographically, the seizures began with a generalized burst of sharp waves followed by sharp wave complexes that were maximal in mesial temporal leads. The patient subsequently underwent a left temporal lobectomy. Pathological examination of the tissue revealed mild dysplastic changes in the lateral temporal neocortex and gliosis and moderate neuronal loss in regions CA4 and CA3 of the hippocampus. Thirteen months after his surgery, he remains seizure free.

Participant C. Participant C was a right-handed woman 22 years old at the time of the continuous 8-d video and invasive EEG monitoring. She had a history of partial seizures with rapid generalization beginning around 14 years of age and typically suffered four to seven attacks per day. Several different clinical manifestations of her seizures had been observed, including events that would occur out of sleep and consist of screaming and whole body shaking. She also had spells of staring, unresponsiveness and oral automatisms. These occasionally progressed to generalized tonic-clonic activity or atonia. Imaging studies including MRI and PET showed diffuse atrophy and questionable abnormalities in the right frontal lobe. Previous EEG monitoring suggested a right-sided region of epileptogenesis, emanating from the either the right frontal or temporal lobe, so she was implanted with extensive subdural coverage of the right hemisphere. The NeuroPort array was implanted in the middle frontal gyrus within a broad onset region.

There were a total of 30 definite seizures throughout the recording session. Each clinical seizure was characterized by a subtle head turn and drop to the right or left that lasted 10–15 s. Electrographically, the seizures fell into four different groups depending on the presence of generalized EEG spikes as well as the seizure onset evolution. The seizures incorporated into our analysis are described in detail below:

Seizure 1 began with an onset of generalized epileptiform spiking activity, followed by 1–2 s of generalized attenuation and then prominent spike and wave activity. Clinically, the subtle head turn corresponded to the generalized EEG spike discharges. The electrographic seizure lasted approximately 11 s.

Seizure 2 started with a generalized EEG spike followed by 1–2 s of attenuation and then the onset of a generalized, high-frequency buzz lasting 4 s. This was followed by EEG spike and wave discharges in the frontopolar strip, the subfrontal strip and segments of the grid of electrodes, lasting 5 s. The seizure corresponded clinically to subtle head movements after the onset of the seizure. The electrographic seizure lasted approximately 11 s.

At the conclusion of the study the patient underwent resection of the left temporal lobe. Pathology confirmed the lesion to be a cortical dysplasia. Six months after surgery the patient had experienced a reduction in the overall number of seizures but continued to have episodes of behavioral arrest.

Participant D. Participant D was a right-handed woman 24 years old at the time of the continuous 4-d video and invasive EEG monitoring study. She had a history of complex partial seizures beginning at the age of fourteen. Her seizures tended to present with staring spells, gulping sounds, a general feeling of heat and hand automatisms. She often had no awareness of the events. Previous EEG monitoring suggested that these seizures originated from the left anterior temporal region. MRI showed a large lesion in the left temporal lobe, believed to be a glioma. In accordance with the above findings, the patient was implanted with a combination of subdural and depth electrodes focused on the left temporal region. The NeuroPort research electrode was placed in the middle temporal gyrus about 2 cm posterior to the temporal tip. The distance to the nearest ECoG electrode where seizure onsets were detected was ~4 cm.

There were five electrographic seizures captured over the course of the 4-d recording session: three typical clinical seizures lasting 20–40 s and two subclinical seizures of shorter duration. The three clinical seizures manifested with staring spells and the participant's report of a general sensation of heat. The EEG revealed the electrographic onset for each of these seizures in the anterior temporal region with a typical subsequent spread across the superior and middle anterior strip electrodes, as well as to the depth electrodes.

At the conclusion of the study, the patient underwent a left anterior temporal lobectomy, a left amygdalohippocampectomy and a lesionectomy of the posterior temporal lobe. Pathology determined the lesion to be a low-grade glioneuronal tumor. At last evaluation, 6 months after surgery, the patient was seizure free.

Microelectrode array location, recordings and analysis. Approval for these studies was granted by local Institutional Review Boards (Partners Human Research Committee) and participants were enrolled after informed consent was obtained. The implanted NeuroPort array (Blackrock Microsystems), which has been used in several previous studies[26–31], is a 4 mm × 4 mm microelectrode array composed of 100 platinum-tipped silicon probes. Arrays with 1.0-mm

doi:10.1038/nn.2782

electrode lengths were implanted in the middle frontal gyrus (participant C) and middle temporal gyrus (participants A, B and D). The array's distance to the nearest ECoG electrode containing seizure onsets, calculated using MRI and post-operative computed tomography registration, was calculated as ~2 cm in participants A and B, ~4 cm in participant D, and within a broad seizure onset zone for participant C. Histology after resection confirmed that the tips of the electrodes were in the lower portion of layer III in two of the three cases (A and B). In these two cases, the histology around the array appeared normal. In a third participant (D), the histology of the cortex also appeared normal but the exact path of the electrode could not be reconstructed. In the fourth participant (C), the array was placed in an area of cortex that was the suspected focus and looked abnormal on visual inspection during the time of the initial craniotomy. Ultimately, however, this area was not resected. For detection and extraction of extracellularly recorded action potentials, the analog signal (0.3 Hz–7.5 kHz) from each of the 96 active electrodes was sampled at 30 kHz, online digitally high-pass filtered (250 Hz–7.5 kHz, fourth-order Butterworth filter) and automatically amplitude thresholded (Cerebus system, Blackrock Microsystems). The extracted waveforms were sorted using standard methods[40] and Offline Sorter (Plexon) and were tracked to ensure that spike rate changes were not obvious artifacts due to waveform changes. Spike sorting was performed on projections of waveforms into feature spaces given by principal components and a nonlinear energy measure. (This nonlinear energy measure is akin to the product of the raw amplitude times the derivative of the signal; Offline Sorter User Guide, version 3, Plexon). In the case of consecutive seizures occurring within ~1 h, we were able to track the neuronal spike waveforms and ensure that the same unit was being isolated. Single-neuron bursting rates were computed as previously described[41]. Classification of neurons into putative interneurons or principal cells[42] was based on neuronal spike waveforms extracted after offline high-pass filtering (forward-backward Kaiser filter, 250 Hz high-pass cutoff) of the original data. Local field potentials were low-pass filtered at 250 Hz. The probability that Pearson correlation coefficients were statistically different from 0 was computed using the Matlab function corrcoef.m (MathWorks).

38. Delgado-Escueta, A.V. & Walsh, G.O. The selection process for surgery of intractable complex partial seizures: surface EEG and depth electrography. in *Epilepsy* (eds. Ward, A.A. Jr., Penry, J.K. & Purpura, D.P.) 295–326 (Raven, New York, 1983).
39. Engel, J., Crandall, P.H. & Rausch, P. Surgical treatment of partial epilepsies. in *The Clinical Neurosciences* (eds. Rosenburg, R.N., Grossman, R.G. & Schoclet, S.) 1349–1380 (Churchill Livingston, New York, 1983).
40. Lewicki, M.S. A review of methods for spike sorting: the detection and classification of neural action potentials. *Network* **9**, 53–78 (1998).
41. Staba, R.J., Wilson, C.L., Bragin, A., Fried, I. & Engel, J. Jr. Sleep states differentiate single neuron activity recorded from human epileptic hippocampus, entorhinal cortex, and subiculum. *J. Neurosci.* **22**, 5694–5704 (2002).
42. Barthó, P. *et al.* Characterization of neocortical principal cells and interneurons by network interactions and extracellular features. *J. Neurophysiol.* **92**, 600–608 (2004).